

# Signal Recovery in Perturbed Fourier Compressed Sensing

Eeshan Malhotra, *Student Member, IEEE*, Himanshu Pandotra, Ajit Rajwade, *Member, IEEE* and Karthik S. Gurumoorthy

**Abstract**—In many applications in compressed sensing, the measurement matrix is a Fourier matrix, *i.e.*, it measures the Fourier transform of the underlying signal at some specified frequencies  $\{u_i\}_{i=1}^M$ , where  $M$  is the number of measurements. However due to system calibration errors, the system may measure the Fourier transform at frequencies  $\{u_i + \delta_i\}_{i=1}^M$  that are different from the specified (known) ‘base’ frequencies. Ignoring perturbations of this nature can lead to major errors in signal recovery. In this paper, we present a simple but effective alternating minimization algorithm to recover the perturbations in the frequencies *in situ* with the signal, which we assume is sparse or compressible in some known basis. We demonstrate that assuming that the number of *unique* perturbations  $\{\delta_i\}_{i=1}^M$  is less than  $M$ , the method leads to excellent quality results that are several times better than baseline algorithms and other related algorithms in the literature, besides being robust to noise in the measurement values. We also analyze a linearized approximation to the proposed objective function, and prove that it yields a unique solution in almost all cases.

**Index Terms**—Compressed sensing, Fourier measurements, Frequency Perturbation

## I. INTRODUCTION

COMPRESSED sensing (CS) is today a very widely researched branch of signal and image processing. Given a vector of compressive measurements  $\mathbf{y} \in \mathbb{C}^M$  acquired through a sensing matrix  $\Phi \in \mathbb{C}^{M \times N}$ , CS theory offers guarantees on the error of reconstruction of a signal  $\mathbf{x} \in \mathbb{C}^N$  that is sparse or compressible in a given orthonormal basis  $\Psi \in \mathbb{C}^{N \times N}$ , assuming that the sensing matrix (also called measurement matrix)  $\Phi \in \mathbb{C}^{M \times N}$  (and hence the product matrix  $\Phi\Psi$ ) obeys some properties such as the restricted isometry (RIP) [1]. Moreover, the guarantees apply to efficient algorithms such as basis pursuit. However the underlying assumption is that the sensing matrix  $\Phi$  is known accurately. If  $\Phi$  is known inaccurately, then signal-dependent noise will be introduced in the system causing substantial loss in reconstruction accuracy.

Of particular interest in many imaging applications such as magnetic resonance imaging (MRI), radar imaging or Fourier optics [2], [3], [4], [5], is the case where the measurement

matrix is a row-sampled version of the Fourier matrix, where the frequencies may or may not lie on a Cartesian grid of frequencies used in defining the Discrete Fourier Transform (DFT). However, it is well-known that such Fourier measurements are prone to inaccuracies in the acquisition frequencies. This may be due to an imperfectly calibrated sensor, or in case of specific applications such as MRI, due to perturbations introduced by gradient delays in the MRI machine [6], [7], [8].

### A. Relation to Previous Work

The problem we deal with in this paper is a special case of the problem of ‘self-calibration’ where perturbations in the sensing matrix are estimated *in situ* along with estimation of the signal, but applied to the case of Fourier sensing matrices with imperfectly known frequencies. There exists a decent-sized body of earlier literature on the general self-calibration problem (not applied to Fourier matrices) beginning with theoretical bounds derived in [9]. Further on, [10] analyze a structured perturbation model of the form  $\mathbf{y} = (\mathbf{A} + \mathbf{B}\Delta)\mathbf{x}$  where  $\mathbf{x}, \Delta$  are the unknown signal and diagonal matrix of perturbation values respectively, and  $\mathbf{A}, \mathbf{B}$  are the fully known original sensing matrix and perturbation matrix respectively. The theory is then applied to direction of arrival (DOA) estimation in signal processing. Further work in [11] uses the notion of group-sparsity to infer the signal  $\mathbf{x}$  and the perturbations  $\Delta$  using a convex program based on a first order Taylor expansion of the parametric Fourier sensing matrix. A total least squares framework that also accounts for sparsity of the signal is explored in [12] for a perturbation model of the form  $\mathbf{y} + \mathbf{e} = (\mathbf{A} + \mathbf{E})\mathbf{x}$  where  $\mathbf{e}, \mathbf{E}$  are the additive errors in the measurement vector  $\mathbf{y}$  and measurement matrix  $\mathbf{A}$  respectively. In [13], [14], [15],[16], the following framework is considered:  $\mathbf{y} = \Delta\mathbf{A}\mathbf{x}$ , where  $\Delta$  is a diagonal matrix containing the unknown sensor gains which may be complex,  $\mathbf{x}$  is the unknown sparse signal, and  $\mathbf{A}$  is the known sensing matrix. Both  $\mathbf{x}$  and  $\Delta$  are recovered together via linear least squares in [13], via the lifting technique on a biconvex problem in [14], using a variety of convex optimization tools in [15], and in [16] using a non-convex method. The problem we deal with in this paper cannot be framed as a single unknown phase or amplitude shift unlike these techniques, and hence is considerably different.

Related to (but still distinctly different from) the aforementioned problem of a perturbed sensing matrix, is the problem of a perturbed or mismatched signal representation matrix

Eeshan Malhotra and Ajit Rajwade are with the Department of Computer Science and Engineering at IIT Bombay. Himanshu Pandotra is with the Department of Electrical Engineering at IIT Bombay. Karthik Gurumoorthy is with the International Center for Theoretical Sciences, Bengaluru. The email addresses of the authors are eeshan@gmail.com, angad@ee.iitb.ac.in, ajitvr@cse.iitb.ac.in and karthik.gurumoorthy@icts.res.in respectively. Corresponding author is Ajit Rajwade. Ajit Rajwade acknowledges generous support from IITB seed grant #14IRCCSG012. Karthik Gurumoorthy thanks the AIRBUS Group Corporate Foundation Chair in Mathematics of Complex Systems established in ICTS-TIFR.

$\Psi$  which can also cause significant errors in compressive recovery [17]. This has been explored via alternating minimization in [18] and via group-sparsity in [11]. The problem of estimating a small number of complex sinusoids with off-the-grid frequencies from a subset of regularly spaced samples has been explored in [19]. Note that in [17], [19], [11], [18], the emphasis is on mismatch in the representation matrix  $\Psi$  and *not* in the sensing matrix  $\Phi$ . The problem of *additive* perturbations in both the sensing matrix as well as the representation matrix has been analyzed in [20], using several assumptions on both perturbations. Note that the perturbations in the Fourier sensing matrix do not possess such an additive nature.

To the best of our knowledge, there is no previous work on the analysis of perturbations in a Fourier *measurement* matrix in a *compressive sensing* framework. Some attempts have been made to account for frequency specification errors in MRI, however, most of these require a separate off-line calibration step where the perturbations are measured. However in practice, the perturbations in frequencies may even vary with each measurement, and need not be static. In cases where the correction is made alongside the recovery step, a large number of measurements may be required [21], as the signal reconstruction does not deal with a compressed sensing framework involving  $\ell_q$  ( $q < 1$ ) minimization. The problem of perturbations in the Fourier matrix also occurs in computed tomography (CT). This happens in an indirect way via the Fourier slice theorem, since the 1D Fourier transform of a parallel beam tomographic projection in some acquisition angle  $\rho$  is known to be equal to a slice of the Fourier transform of the underlying 2D image at angle  $\rho$ . In CT, the angles for tomographic projection may be incorrectly known due to geometric errors [22] or subject motion, and uncertainty in the angle will manifest as inaccuracy of the Fourier measurements. Especially in case of subject motion, the measurement matrix will contain inaccuracies that cannot be pre-determined, and must be estimated *in situ* along with the signal. While there exist approaches to determine even the completely unknown angles of projection, they require a large number of angles, and also the knowledge of the distribution of the angles [23], [24]. Our group has presented a method [25] which does not require this knowledge, but in [25], the angles are estimated only along with the image moments. The image itself is estimated after determining the angles. In contrast, in this paper, the errors in frequency are determined along with the underlying signal.

A large body of existing work is also lacking in theoretical backing. For instance [20] makes assumptions on the properties of the perturbed measurement matrix, such as the magnitudes of the perturbations. Some existing approaches simplify the problem using a Taylor approximation [11], [10]. However, such a reduction proves to be adequate only at extremely small perturbation levels in our case, rendering the adjustment for the perturbation to be much less effective (See Section IV).

**Contributions:** A method for simultaneous recovery of the perturbations and the signal in a perturbed Fourier compressed sensing structure is proposed in this paper. The algorithm is verified empirically over a large range of simulated data under

noise-free and noisy cases. Further, a theoretical backing is provided for the method that provides bounds on the expected perturbed Fourier matrix, and probabilistic guarantees on the recovered signal given a linearized approximation of the original objective function.

## B. Organization of the Paper

This paper is organized as follows. Section II defines the problem statement. The recovery algorithm is presented in Section III, followed by extensive numerical results in Section IV. The theoretical treatment is covered in Section V, followed by a conclusion in Section VI

## II. PROBLEM DEFINITION

Formally, let  $\mathbf{F} \in \mathbb{C}^{M \times N}$  be a Fourier matrix using a known (possibly, but not necessarily on-grid) frequency set  $\mathbf{u} \triangleq \{u_i\}_{i=1}^M \in \mathbb{R}^M$ ,  $\mathbf{x} \in \mathbb{R}^N$  be a signal that is sparse (with at the most  $s$  non-zero values) or compressible, measured using a perturbed Fourier matrix  $\mathbf{F}_t \in \mathbb{C}^{M \times N}$ . That is,

$$\mathbf{y} = \mathbf{F}_t \mathbf{x} + \boldsymbol{\eta},$$

where,  $\mathbf{F}_t$  is a Fourier measurement matrix at the set of unknown frequencies  $\mathbf{u} + \boldsymbol{\delta} \triangleq \{u_i + \delta_i\}_{i=1}^M$ , with  $\forall i, \delta_i \in \mathbb{R}, |\delta_i| \leq r, r \geq 0$ . Note that we assume full knowledge of  $\{u_i\}_{i=1}^M$ , *i.e.*, the base frequencies. The problem is to recover *both*, the sparse signal  $\mathbf{x}$ , and the unknown perturbations in the frequencies,  $\boldsymbol{\delta}$ . This is formalized as the objective:

$$\min_{\hat{\mathbf{x}}, \hat{\boldsymbol{\delta}} \in [-r, r]^M} \|\hat{\mathbf{x}}\|_1 + \lambda \|\mathbf{y} - \hat{\mathbf{F}} \hat{\mathbf{x}}\|_2 \quad (1)$$

where  $\hat{\mathbf{F}}$  is the Fourier measurement matrix at frequencies  $\mathbf{u} + \hat{\boldsymbol{\delta}}$ , and  $\hat{\boldsymbol{\delta}}$  denotes the estimate of  $\boldsymbol{\delta}$ . Note that the above problem is a perturbed version of the so-called square-root LASSO (SQ-LASSO), since the second term involves an  $\ell_2$  norm and not its square. We used the SQ-LASSO due to its advantages over the LASSO, as mentioned in [26].

Eqn. II presents the most general formulation of the problem. We also discuss two modifications, both of which are also solved by a small modification of the same recovery algorithm.

First, in Eqn. II, we have assumed that all perturbations, *i.e.* entries in  $\boldsymbol{\delta}$  are independent. However, this may not necessarily be the case. For example, in radial 2-D MR imaging, all Fourier measurements along a radial spoke in a given direction may suffer from the same (or related) perturbations, and thus the number of perturbation parameters is equal to the number of spoke angles. This is also true of a variety of other protocols in MR imaging. Handling this is easy and in fact, makes the recovery problem more tractable, since the number of unknowns is essentially reduced. Second, the signal may be sparse in a non-canonical basis - say Discrete wavelet transform (DWT). This can also be easily incorporated in the recovery algorithm, as discussed in the next section.

## III. RECOVERY ALGORITHM

We present an algorithm to determine  $\mathbf{x}$  and  $\boldsymbol{\delta}$  by using an alternation between two sub-problems. Starting with a guess for the perturbations  $\hat{\boldsymbol{\delta}}$ , we recover  $\hat{\mathbf{x}}$ , an estimate for  $\mathbf{x}$ , using

an unconstrained  $l_1$  norm minimization approach common in compressive sensing [27]. Next, using this first estimate  $\hat{\mathbf{x}}$ , we update  $\hat{\boldsymbol{\delta}}$  to be the best estimate, assuming  $\hat{\mathbf{x}}$  to be the truth, using a linear brute force search in the range  $-r$  to  $r$ . A linear search is possible because each measurement  $y_i$  is the dot product of a single row of  $\mathbf{F}_t$  with  $\mathbf{x}$ , and hence a single  $(u_i, \delta_i)$  value is involved. Consequently, the different  $\delta_i$  values can be recovered through *independent* parallel searches. This is quite unlike the basis mismatch problem in [18] where the perturbations in the *signal representation basis vectors* (not the measurement matrix) have to be jointly optimized, unless the representation matrix is (approximately) orthogonal. From here on, we alternate between the two steps - recovery of  $\hat{\mathbf{x}}$  and  $\hat{\boldsymbol{\delta}}$ , till convergence is achieved. Note that the regularization parameter  $\lambda$  in Eqn. II was chosen by cross-validation on a small ‘training set’ of signals.

Since the search space is highly non-convex, we also employ a multi-start strategy, where, we perform multiple runs of the alternating algorithm to recover  $\hat{\boldsymbol{\delta}}$  and  $\hat{\mathbf{x}}$ , each time, initializing the first guess for  $\hat{\boldsymbol{\delta}}$  randomly. We ultimately select the solution that minimizes the objective function, i.e.,  $\|\hat{\mathbf{x}}\|_1 + \lambda \|\mathbf{y} - \hat{\mathbf{F}}\hat{\mathbf{x}}\|_2$ . In practice, we have observed that the number of runs required for a good quality solution is rather small (around 10).

The full algorithm, including the optimization for multi-start is presented in Algorithm 1.

---

**Algorithm 1** Alternating Minimization Algorithm
 

---

```

1: procedure ALTERNATIVERECOVERY
2:   converged  $\leftarrow$  False
3:    $\hat{\boldsymbol{\delta}} \leftarrow$  sample from Unif $[-r, +r]$ 
4:   while converged == False do
5:      $\hat{\mathbf{F}} \leftarrow$  Fourier matrix at  $(\mathbf{u} + \hat{\boldsymbol{\delta}})$ 
6:     Estimate  $\hat{\mathbf{x}}$  as:
7:      $\min_{\hat{\mathbf{x}}} \|\hat{\mathbf{x}}\|_1 + \lambda \|\mathbf{y} - \hat{\mathbf{F}}\hat{\mathbf{x}}\|_2$ 
8:
9:     for  $k$  in  $1 \rightarrow M$  do
10:      Test each discretized value of  $\hat{\delta}_k$  in range
       $-r$  to  $r$  and select the value to achieve  $\min_{\hat{\delta}_k} \|\mathbf{y}_k - \hat{\mathbf{F}}_k \hat{\mathbf{x}}\|_2$ 
11:      if  $\|\hat{\boldsymbol{\delta}} - \hat{\boldsymbol{\delta}}_{prev}\|_2 < 1e-4$  and
       $\|\hat{\mathbf{x}} - \hat{\mathbf{x}}_{prev}\|_2 < 1e-4$  then
12:        converged  $\leftarrow$  True
13:      return  $\hat{\mathbf{x}}, \hat{\boldsymbol{\delta}}$ 

14: procedure MULTISTART
15:   minobjective  $\leftarrow$   $\infty$ 
16:    $\hat{\mathbf{x}}_{best} \leftarrow$  null
17:    $\hat{\boldsymbol{\delta}}_{best} \leftarrow$  null
18:   for start in  $1 \rightarrow$  numstarts do
19:      $\hat{\mathbf{x}}, \hat{\boldsymbol{\delta}} \leftarrow$  AlternatingRecovery()
20:      $\hat{\mathbf{F}} \leftarrow$  Fourier matrix at  $(\mathbf{u} + \hat{\boldsymbol{\delta}})$ 
21:     objective  $\leftarrow$   $\|\hat{\mathbf{x}}\|_1 + \lambda \|\mathbf{y} - \hat{\mathbf{F}}\hat{\mathbf{x}}\|_2$ 
22:     if objective < minobjective then
23:        $\hat{\mathbf{x}}_{best} \leftarrow$   $\hat{\mathbf{x}}$ 
24:        $\hat{\boldsymbol{\delta}}_{best} \leftarrow$   $\hat{\boldsymbol{\delta}}$ 
25:     minobjective  $\leftarrow$  objective
26:   return  $\hat{\mathbf{x}}_{best}, \hat{\boldsymbol{\delta}}_{best}$ 

```

---

To handle cases where values in  $\hat{\boldsymbol{\delta}}$  are shared among a subset of indices, we can replace step 9 in Algorithm 1. Consider  $P \ll M$  unique values in  $\hat{\boldsymbol{\delta}}$  with the  $k^{\text{th}}$  unique value corresponding to a set of indices  $L_k$  (indexing into the measurement vector  $\mathbf{y}$ ). Step 9 can then be replaced by:

**for**  $k$  in  $1 \rightarrow P$  **do**

Test each discretized value of  $\hat{d}_k$  in range  $-r$  to  $r$

Select the value to achieve  $\min_{\hat{d}_k} \|\mathbf{y}_{L_k} - \hat{\mathbf{F}}_{L_k} \hat{\mathbf{x}}\|_2$

**for each**  $l$  in  $L_k$  **do**

$\delta_l \leftarrow \hat{d}_k$

In the above steps,  $\mathbf{y}_{L_k}$  is a subvector of  $\mathbf{y}$ , containing measurements for frequencies at indices only in  $L_k$ , and  $\hat{\mathbf{F}}_{L_k}$  denotes a submatrix of  $\hat{\mathbf{F}}$  containing only those rows with indices in  $L_k$ . Note that the modification to the main algorithm essentially computes only each *unique* value in  $\boldsymbol{\delta}$  separately. The algorithm can be easily extended to the case where the signal  $\mathbf{x}$  is sparse/compressible in some orthonormal basis  $\boldsymbol{\Psi} \neq \mathbf{I}$ , by simply replacing  $\hat{\mathbf{F}}\mathbf{x}$  by  $\hat{\mathbf{F}}\boldsymbol{\Psi}\boldsymbol{\theta}$ . Since at each step, the objective function monotonically decreases, and yet, is bound to be non-negative, the alternating algorithm is guaranteed to converge.

## IV. EMPIRICAL RESULTS

### A. Recovery of 1-D signals

We present recovery results on signals in a multitude of cases below. In each chart (see Figures 1,2,3,4), 1D signals of  $N = 101$  elements were used, the sparsity  $s$  of the signal was varied along the x-axis, and the number of measurements  $M$  was varied along the y-axis. The cell at the intersection depicts the recovery error,  $\frac{\|\mathbf{x} - \hat{\mathbf{x}}\|_2}{\|\mathbf{x}\|_2}$ , averaged across 5 different signals. The  $M$  compressive measurements for the signals were randomly chosen from  $-N/2$  to  $N/2$ . All cases had different perturbations chosen from Unif $[-r, +r]$ , for two separate cases with  $r = 1$  and  $r = 0.5$  respectively. See Section II for the meaning of  $r$ . Black (RGB (0,0,0)) indicates perfect recovery, and white (RGB (1,1,1)) indicates recovery error of 100% or higher. Note that all the figures show error values plotted on the same scale, and hence the shades are comparable within and across figures. In all experiments, a multi-start strategy with 10 starts was adopted. In principle, the bound  $r = 0.5$  avoids ambiguity in the estimation of the  $\boldsymbol{\delta}$  values as compared to  $r = 1$ . However even the latter does not have any major adverse effect on the signal reconstruction.

Figure 1 shows results for two different cases (top and bottom figures, for both  $r = 1$  and  $r = 0.5$ ): where the number of unique values in  $\boldsymbol{\delta}$  are 2 and 10 respectively (this is henceforth denoted as  $\delta_{(u)}$ ), although there are  $M$  measurements. In both cases, no external noise was added to the measurements. One can see that the average recovery error decreases with the number of measurements and increases with increase in  $s$ , although the relationship is not strictly monotonic. Figure 2 shows the same two cases as in Figure 1, but with an addition of zero mean i.i.d. Gaussian noise with  $\sigma = 5\%$  of the average magnitude of the individual measurements. The same trend of

decrease in error with increased number of measurements and increase in error with increased  $s$  is observed here as well. For reference, we also include a typical sample reconstruction in 1D canonical basis for a signal of length 101, which is 10-sparse, in Figure 6. Figure 3 shows similar results as in Figure 2 but using signals that are sparse in the Haar wavelet basis instead of the canonical basis.

### B. Baselines for Recovery of 1-D signals

For comparison, we also establish two baselines:

- 1) A naive reconstruction algorithm, which ignores the perturbations and recovers the signal using a straightforward basis pursuit approach, with the *unperturbed, on-grid* Fourier matrix as the measurement matrix, i.e. assuming  $\delta = \mathbf{0}$ . Results in similar settings as in Figure 1 are shown in Figure 4.
- 2) A Taylor approximation approach: Here, the signal as well as the perturbations are recovered using an alternating minimization algorithm based on a first order Taylor approximated formulation. That is,

$$\mathbf{y} = \mathbf{F}_t \mathbf{x} \approx (\mathbf{F} + \Delta \mathbf{F}') \mathbf{x} + \boldsymbol{\eta}_{Taylor}, \quad (2)$$

where  $\mathbf{F}$  represents the Fourier measurement matrix at known frequency set  $\{u_i\}_{i=1}^M$ ,  $\mathbf{F}'$  represents its derivative w.r.t.  $\delta$ ,  $\Delta \triangleq \text{diag}(\delta)$ , and  $\boldsymbol{\eta}_{Taylor}$  represents the error due to truncation in the Taylor series. Results in similar settings as in Figure 1 are shown in Figure 5 for two cases: one where the number of unique values in  $\delta$  is two, and another where it is ten.

As is clear from the figures, Baseline 1 performs considerably worse, since inaccurate frequencies are trusted to be accurate. Baseline 2 *also* performs badly because the first order Taylor error,  $\boldsymbol{\eta}_{Taylor}$ , can be overwhelmingly large since it is directly proportional to the unknown  $\|\mathbf{x}\|_2$ , and consequently, the signal recovered is also inferior. In fact, a comparison between Figures 4 and 5 reveals that in case of Taylor approximations to a perturbed Fourier matrix, the results obtained are often as bad as those obtained when assuming  $\delta = \mathbf{0}$ . Baseline 2 is akin to a strategy used in [11], [10] and applied to DOA estimation in radar. However the specific inverse problem to be solved in [11], [10] was more similar to a problem of mismatched representation bases, which fortuitously allowed for joint sparsity of  $\mathbf{x}$  and  $\delta \cdot \mathbf{x}$ , which cannot be achieved in the problem we attempt to solve in this paper.

All the experiments so far were conducted in the setting where the number of unique values in  $\delta$  was much less than  $M$ . In further experiments, we also observed that if the number of unique values in  $\delta$  is equal to  $M$ , it does indeed adversely affect the performance of the alternating minimization algorithm, yielding signal recovery errors that are unacceptably large.

### C. Recovery of 2-D signals

Extension of the algorithm to two dimensions is natural and more immediately applicable to MRI, and we present proof-

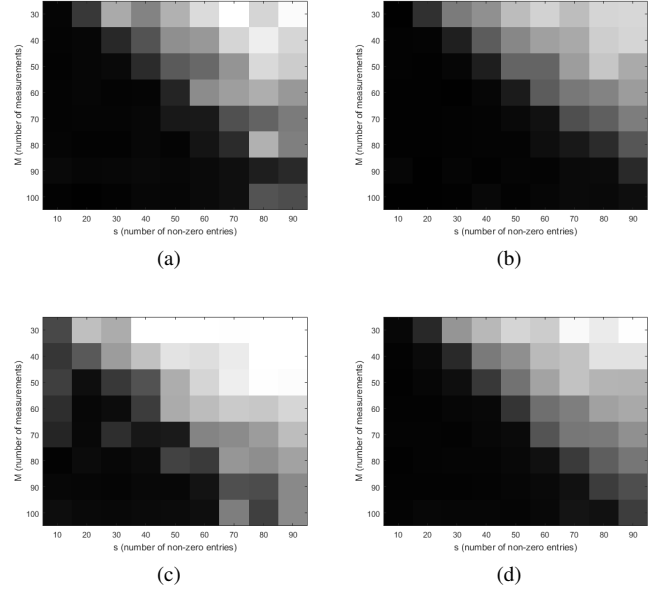


Figure 1. Recovery with Proposed Alternating Minimization algorithm for a 1D signal with 101 elements, sparse in canonical basis, no measurement noise added (a)  $r = 1, \delta_{(u)} = 2$ , (b)  $r = 0.5, \delta_{(u)} = 2$ , (c)  $r = 1, \delta_{(u)} = 10$ , (d)  $r = 0.5, \delta_{(u)} = 10$ , where  $\delta_{(u)}$  represents number of unique values in  $\delta$ .

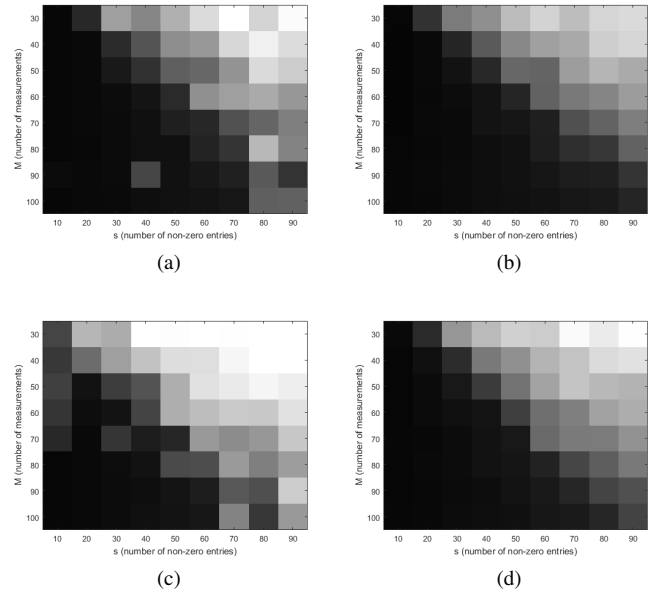


Figure 2. Recovery with Proposed Alternating Minimization algorithm for a 1D signal with 101 elements, sparse in canonical basis, zero mean Gaussian noise added to measurements. (a)  $r = 1, \delta_{(u)} = 2$ , (b)  $r = 0.5, \delta_{(u)} = 2$ , (c)  $r = 1, \delta_{(u)} = 10$ , (d)  $r = 0.5, \delta_{(u)} = 10$ , where  $\delta_{(u)}$  represents number of unique values in  $\delta$ .

of-concept results with a similar set of experiments using two-dimensional images as the signal  $\mathbf{x}$ , which was sparse in the Haar Wavelet Transform (HWT) basis.

For this proof-of-concept experiment, a  $30 \times 30$  pixels image was used, that is sparse in the HWT basis. We utilised a radial sampling approach in the Fourier domain, taking a fixed number of measurements along each spoke, but varying the number of angles used, as well as the sparsity of the image

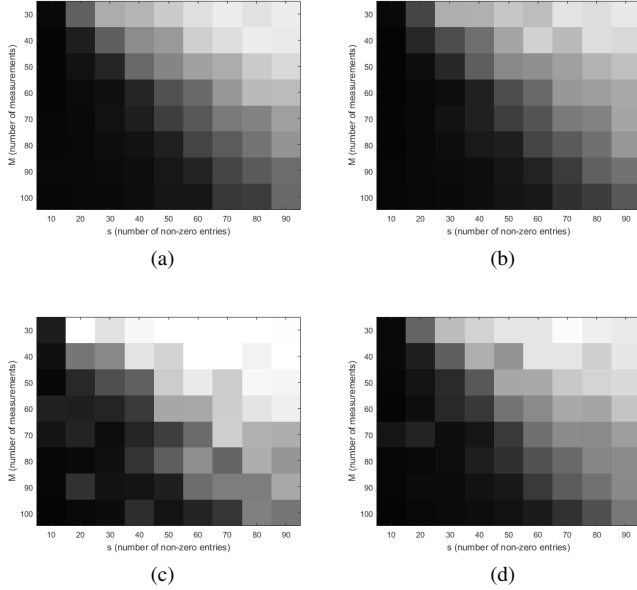


Figure 3. Recovery with Proposed Alternating Minimization algorithm for a 1D signal with 128 elements, sparse in Haar DWT basis, zero mean Gaussian noise added to the measurements. (a)  $r = 1, \delta_{(u)} = 2$  (b)  $r = 0.5, \delta_{(u)} = 2$  (c)  $r = 1, \delta_{(u)} = 10$ , (d)  $r = 0.5, \delta_{(u)} = 10$ , where  $\delta_{(u)}$  represents number of unique values in  $\delta$ .

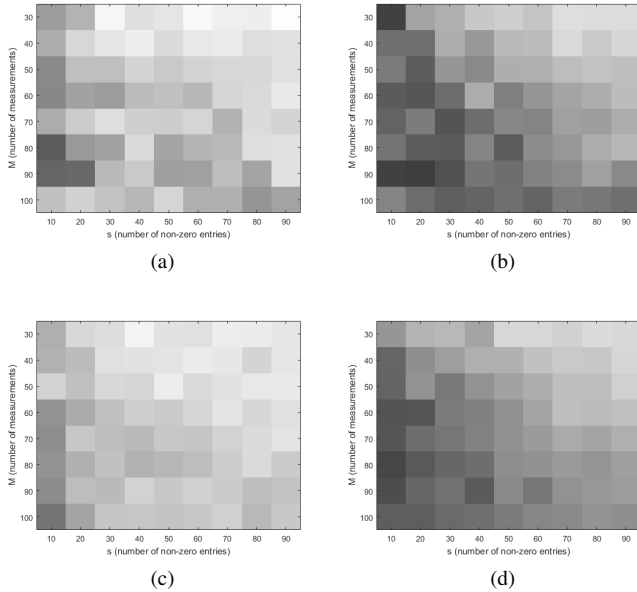


Figure 4. Recovery with Baseline 1 algorithm (see text) for a 1D signal with 101 elements, sparse in canonical basis, no measurement noise added. (a)  $r = 1, \delta_{(u)} = 2$ , (b)  $r = 0.5, \delta_{(u)} = 2$ , (c)  $r = 1, \delta_{(u)} = 10$ , (d)  $r = 0.5, \delta_{(u)} = 10$ , where  $\delta_{(u)}$  represents number of unique values in  $\delta$ . Compare to Figure 1.

in the HWT basis. In addition, 5% zero mean i.i.d. Gaussian noise was added to the measurements (both real and complex parts, independently). The results are summarized in a chart shown in Figure 7. As Figure 7 shows, the recovery error was small, even for a reasonably small number of measurements, and the method was robust to noise in the measurements. We also include a sample reconstructed 2D signal - a  $30 \times 30$

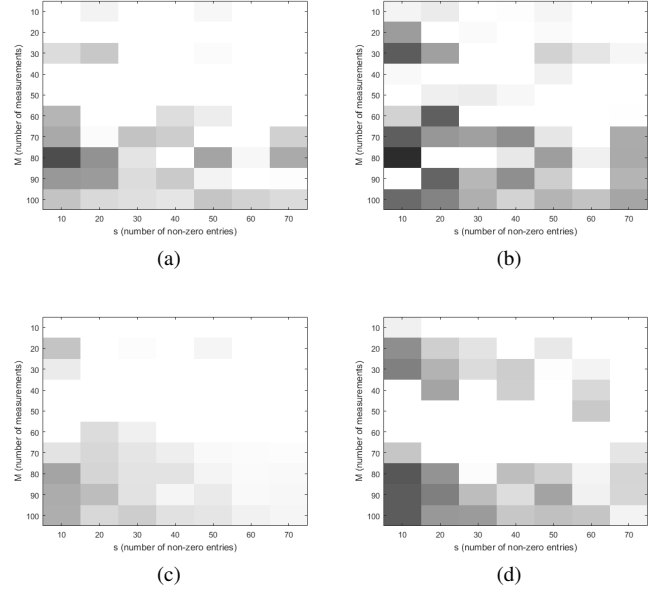


Figure 5. Recovery with Baseline 2 algorithm (see text) for a 1D signal with 101 elements, sparse in canonical basis, zero mean Gaussian noise added to measurements. (a)  $r = 1, \delta_{(u)} = 2$ , (b)  $r = 0.5, \delta_{(u)} = 2$ , (c)  $r = 1, \delta_{(u)} = 10$ , (d)  $r = 0.5, \delta_{(u)} = 10$ , where  $\delta_{(u)}$  represents number of unique values in  $\delta$ . Compare with Figure 2.

pixels image reshaped to a 1-D signal of length 900. The original and recovered signal, along with the error are both presented in Figure 8.

## V. THEORETICAL RESULTS

While the empirical results show the algorithm working well across a large number of simulated scenarios, we also characterize the formulation by providing some theoretical bounds.

### A. Coherence of Perturbed Fourier Matrix

There exist results from the compressed sensing literature that derive performance bounds on signal reconstruction in terms of the mutual coherence of the sensing matrix  $\Phi$  [28]. We provide a bound on the mutual coherence (hereafter simply referred to as ‘coherence’) of the perturbed Fourier matrix, and subsequently prove this bound.

*Theorem 1:* Let  $F_t$  be the Fourier matrix at frequencies  $\mathbf{u} + \delta$ , where  $\mathbf{u}$  represents (the possibly but not necessarily on-grid) frequency set, and  $\delta \sim \text{Unif}[-r, +r], r > 0$  represents the perturbation to this set. Then, the coherence  $\mu_t$  of  $F_t$ , in expectation, is given by:

$$\mu_t \leq \max_{\theta} \mu \frac{|\sin(\theta r)|}{\theta r} \leq \mu$$

where  $\mu$  is the coherence of the unperturbed, row-subsampled Fourier matrix  $F$ , and  $\theta$  takes values  $\frac{2\pi(j_1 - j_2)}{N}$ , for  $j_1 \neq j_2, j_1 \in \{0, 1, \dots, N - 1\}, j_2 \in \{0, 1, \dots, N - 1\}$ .

Since the coherence of the perturbed matrix can be shown to be close to the unperturbed Fourier matrix (in expectation),

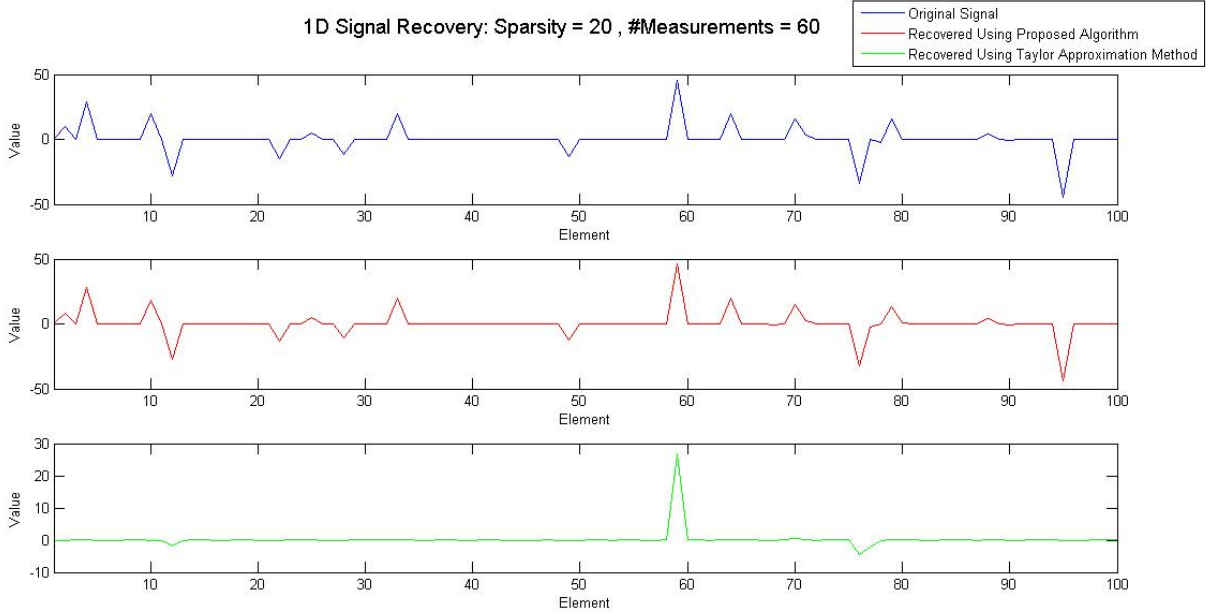


Figure 6. Sample recovered signal error for 1D image sparse in canonical basis, 5% Gaussian noise. Relative reconstruction error by proposed algorithm: 5.5%. Relative reconstruction error by taylor approximation method: 88.7%.

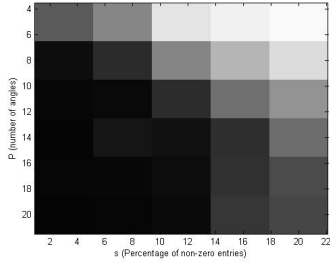


Figure 7. Recovery error for  $30 \times 30$  2D image, sparse in Haar Wavelet basis, with 5% zero mean Gaussian measurement noise

which is low, even in a row-sampled Fourier matrix (i.e.  $M \leq N$ ), we can call upon well-established compressive sensing results to show that the problem is well-founded in theory.

We now prove theorem 1. The expected coherence of  $\mathbf{F}_t$  is found under the assumption that each  $\delta_k$  is drawn i.i.d. from  $\text{Unif}[-r, +r]$ . For notational convenience, we will replace  $\mathbf{F}_t$  by  $\mathbf{F}$  in this subsection only.

The  $(k, j)^{th}$  entry in  $\mathbf{F}$  is given by:

$$F_{k,j} = \frac{1}{\sqrt{N}} \exp\left(\frac{-i2\pi j(u_k + \delta_k)}{N}\right), \quad (3)$$

where  $j \in \{0, 1, \dots, N-1\}$  represents the spatial coordinate,  $k \in \{0, 1, \dots, M-1\}$  represents the index for the frequency coordinate, and  $i = \sqrt{-1}$ .

The coherence of  $\mathbf{F}$  is given by:

$$\max_{j_1 \neq j_2} |F_{:,j_1}^H F_{:,j_2}| \quad (4)$$

where  $H$  stands for the conjugate transpose. Consider the quantity inside the modulus. This is a function of  $\boldsymbol{\delta}$ . We denote this quantity by  $V(\boldsymbol{\delta})$ .

$$V(\boldsymbol{\delta}) = F_{:,j_1}^H F_{:,j_2} = \frac{1}{N} \sum_k \exp\left(\frac{i2\pi(j_1 - j_2)(u_k + \Delta_k)}{N}\right). \quad (5)$$

Let  $\theta = \frac{2\pi(j_1 - j_2)}{N}$ . Replacing in the equation 5,

$$V(\boldsymbol{\delta}) = \frac{1}{N} \sum_k \exp(i\theta(u_k + \delta_k)). \quad (6)$$

Taking an expectation of  $V$ , we have

$$\begin{aligned} E[V] &= \int_{-r}^r V(\boldsymbol{\delta}) p(\boldsymbol{\delta}) d\boldsymbol{\delta} \\ &= \int_{-r}^r \frac{1}{N} \sum_k \exp(i\theta(u_k + \delta_k)) \frac{1}{2r} d\delta_k \\ &= \frac{1}{N} \sum_k \frac{\exp(i\theta u_k)}{2r} \int_{-r}^r \exp(i\theta \delta_k) d\delta_k. \end{aligned}$$

Since

$$\int_{-r}^r \sin(\theta \delta_k) d\delta_k = 0$$

and

$$\int_{-r}^r \cos(\theta \delta_k) d\delta_k = \frac{2}{\theta} \sin(\theta r),$$

We can write  $E[V]$  as

$$E[V] = \frac{1}{N} \sum_k \frac{\exp(i\theta u_k)}{2r} \frac{2}{\theta} \sin(\theta r) \quad (7)$$

$$= \frac{1}{Nr\theta} \sin(\theta r) \sum_k \frac{\exp(i\theta u_k)}{r}. \quad (8)$$

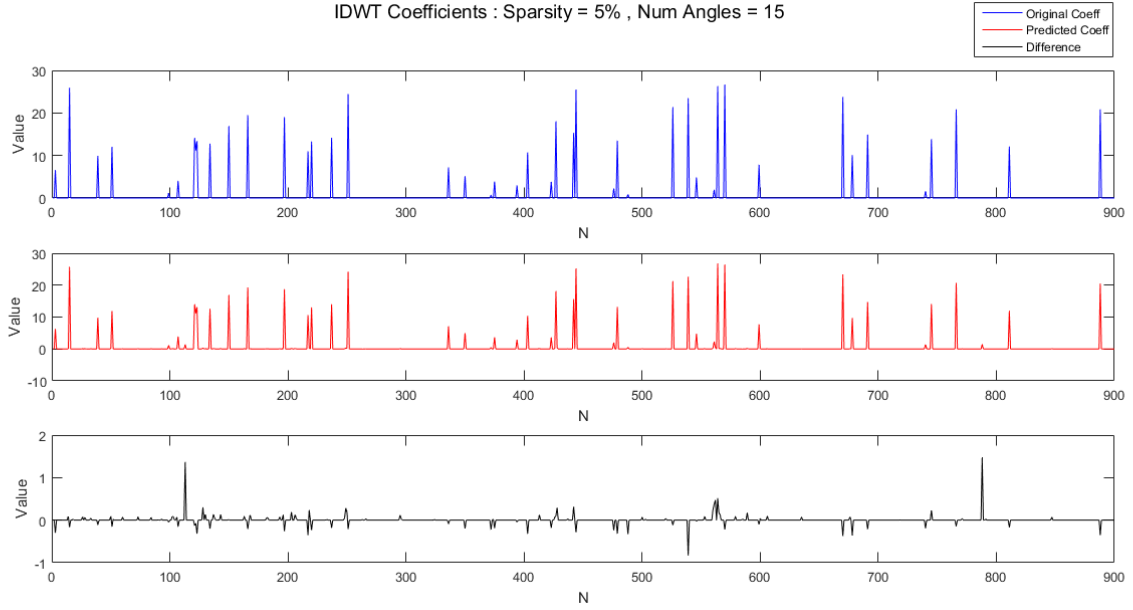


Figure 8. Sample recovered signal error for 2D image sparse in HWT basis (flattened to a 1D vector for visualization purposes), 5% zero-mean Gaussian noise

We know that for any  $k$ ,

$$\frac{1}{N} \left| \sum_k \exp(i\theta u_k) \right| \leq \mu$$

where  $\mu$  is the coherence of the unperturbed Fourier matrix at frequencies  $\mathbf{u}$ . Therefore,  $E[V]$  in equation 8 can be bounded by

$$\mu \frac{\sin(\theta r)}{\theta r} \quad (9)$$

where  $\theta$  takes values  $\frac{2\pi(j_1 - j_2)}{N}$ , for  $j_1 \neq j_2$ .

Since  $\frac{|\sin(\theta r)|}{\theta r}$  is a sinc function, it takes a maximum value of 1. Therefore, the coherence of the perturbed Fourier matrix is less than or equal to the coherence of the unperturbed Fourier matrix in expectation. In practice, the coherence values of the two matrices were found to be extremely close.

### B. Formulation by Taylor Approximation

In this section, we theoretically analyze a first order Taylor approximation of the original objective function in order to provide more insight into the problem. In the following, we consider  $\Delta \triangleq \text{diag}(\delta)$ . Let  $\mathbf{F}$  denote the Fourier matrix at frequencies  $\mathbf{u}$ . We can treat  $\mathbf{F}_t$  as approximated by  $\mathbf{F} + \Delta \mathbf{F}'$ , where  $\mathbf{F}'$  is the derivative of the Fourier matrix with respect to the elements in  $\Delta$ . In other words,

$$\begin{aligned} \mathbf{F}_t &\approx \mathbf{F} + \Delta \mathbf{F}' \\ &\text{with } \mathbf{F}' = \mathbf{F} \mathbf{X} \end{aligned}$$

where  $\mathbf{X}$  is a diagonal matrix, with  $X_{kk} = \frac{2\pi k}{N}$ .

*Theorem 2:* For measurements  $\mathbf{y} \in \mathbb{C}^M$  of the form

$$\mathbf{y} = (\mathbf{F} + \Delta \mathbf{F} \mathbf{X}) \mathbf{x},$$

the signal  $\mathbf{x} \in \mathbb{R}^N$  and the perturbations  $\Delta$  (diagonal  $N \times N$  matrix) can both be uniquely recovered with probability 1, independent of the sparsity of the signal  $\mathbf{x}$  and the magnitude of the values in  $\Delta$ , if (a)  $M = N$ , (b)  $\mathbf{x}$  is neither purely even nor purely odd, and (c)  $\mathbf{y}$  should not contain any pair of elements that are conjugate symmetric.

To prove this, we utilise the following defined relations:

$$\mathbf{F} = \mathbf{C} + i\mathbf{S} \quad (10)$$

$$\mathbf{x} = \mathbf{e} + \mathbf{o} \quad (11)$$

$$\mathbf{y} = \mathbf{y}_r + i\mathbf{y}_c \quad (12)$$

where,  $\mathbf{C}$  is the cosine component and  $\mathbf{S}$  is the sine component of  $\mathbf{F}$ ,  $\mathbf{e}$  is an even component of length  $N$ , and  $\mathbf{o}$  is an odd component of length  $N$ ,  $\mathbf{y}_r$  is the real component of  $\mathbf{y}$ , and  $i\mathbf{y}_c$  is the complex component of  $\mathbf{y}$ . It should be noted that given  $\mathbf{x}$ ,  $\mathbf{e}$  and  $\mathbf{o}$  are uniquely defined.

Therefore,  $\mathbf{y} = (\mathbf{F} + \Delta \mathbf{F} \mathbf{X}) \mathbf{x}$  can be rewritten as:

$$\mathbf{y}_r + i\mathbf{y}_c = \mathbf{C} \mathbf{x} + i\mathbf{S} \mathbf{x} + i\Delta(\mathbf{C} + i\mathbf{S}) \mathbf{X} \mathbf{x},$$

which implies that

$$\mathbf{y}_r = \mathbf{C} \mathbf{x} - \Delta \mathbf{S} \mathbf{X} \mathbf{x}, \text{ and} \quad (13)$$

$$\mathbf{y}_c = \mathbf{S} \mathbf{x} + \Delta \mathbf{C} \mathbf{X} \mathbf{x}. \quad (14)$$

Note that  $\mathbf{C} \mathbf{o} = \mathbf{S} \mathbf{X} \mathbf{o} = \mathbf{S} \mathbf{e} = \mathbf{C} \mathbf{X} \mathbf{e} = \mathbf{0}$ .

$$\text{Let } \mathbf{C} = [\mathbf{C}_{-1} \quad \mathbf{C}_0 \quad \mathbf{C}_1] = \begin{bmatrix} \mathbf{C}_{-1,-1} & \mathbf{C}_{0,-1} & \mathbf{C}_{1,-1} \\ \mathbf{C}_{-1,0} & \mathbf{C}_{0,0} & \mathbf{C}_{1,0} \\ \mathbf{C}_{-1,1} & \mathbf{C}_{0,1} & \mathbf{C}_{1,1} \end{bmatrix}.$$

Similarly,

$$\text{let } \mathbf{S} = \begin{bmatrix} \mathbf{S}_{-1} & \mathbf{S}_0 & \mathbf{S}_1 \end{bmatrix} = \begin{bmatrix} \mathbf{S}_{-1,-1} & \mathbf{S}_{0,-1} & \mathbf{S}_{1,-1} \\ \mathbf{S}_{-1,0} & \mathbf{S}_{0,0} & \mathbf{S}_{1,0} \\ \mathbf{S}_{-1,1} & \mathbf{S}_{0,1} & \mathbf{S}_{1,1} \end{bmatrix}.$$

If the frequencies in  $\mathbf{u}$  form an anti-symmetric set about 0 (as is true for on-grid frequencies from  $-N/2$  to  $N/2$  used in a typical DFT matrix), we further have

$$\begin{aligned} \mathbf{C}_{-1} &= \mathbf{C}_1, & \mathbf{S}_{-1} &= -\mathbf{S}_1, \\ \mathbf{C}_{-1,-1} &= \mathbf{C}_{-1,1}, & \mathbf{S}_{-1,-1} &= -\mathbf{S}_{-1,1}, \\ \mathbf{C}_{1,-1} &= \mathbf{C}_{1,1}, & \mathbf{S}_{1,-1} &= -\mathbf{S}_{1,1}, \end{aligned}$$

$$\mathbf{C}_0 = \begin{bmatrix} 1 \\ 1 \\ \vdots \\ 1 \end{bmatrix}, \text{ and } \mathbf{S}_0 = \begin{bmatrix} 0 \\ 0 \\ \vdots \\ 0 \end{bmatrix}.$$

Separating out  $\mathbf{e}$  and  $\mathbf{o}$  and  $\mathbf{X}$  also in a similar fashion, let

$$\mathbf{e} = \begin{bmatrix} \mathbf{e}_{-1} \\ \mathbf{e}_0 \\ \mathbf{e}_1 \end{bmatrix}, \mathbf{o} = \begin{bmatrix} \mathbf{o}_{-1} \\ \mathbf{o}_0 \\ \mathbf{o}_1 \end{bmatrix} \text{ and } \mathbf{X} = \begin{bmatrix} \mathbf{X}_{-1} & \mathbf{0} & \mathbf{0} \\ \mathbf{0} & \mathbf{0} & \mathbf{0} \\ \mathbf{0} & \mathbf{0} & \mathbf{X}_1 \end{bmatrix} \text{ where } \mathbf{e}_{-1} = \mathbf{e}_1, \mathbf{o}_{-1} = -\mathbf{o}_1 \text{ and } \mathbf{X}_{-1} = -\mathbf{X}_1. \text{ Using these, equations 13 and 14 can be rewritten as:}$$

$$\mathbf{y}_r = 2\mathbf{C}_1\mathbf{e}_1 + \mathbf{C}_0\mathbf{e}_0 - \mathbf{\Delta}(2\mathbf{S}_1\mathbf{X}_1\mathbf{e}_1) \quad (15)$$

and

$$\mathbf{y}_c = 2\mathbf{S}_1\mathbf{o}_1 + \mathbf{\Delta}(2\mathbf{C}_1\mathbf{X}_1\mathbf{o}_1).$$

When  $\mathbf{x}$  is purely even ( $\mathbf{o}_1 = \mathbf{0}$ ) or purely odd ( $\mathbf{e}_1 = \mathbf{0}$ ), then  $\mathbf{y}_c$  or  $\mathbf{y}_r$  is respectively zero and we have  $N + \lceil N/2 \rceil$  unknown quantities to solve using  $N$  known values of either  $\mathbf{y}_r$  or  $\mathbf{y}_c$ . Clearly, we do not have uniqueness. Consequently, we require assumption (b) in the theorem. Using 15, the middle component  $y_{r0}$  is given by:

$$y_{r0} = 2\mathbf{C}_{1,0}\mathbf{e}_1 + \mathbf{C}_{0,0}\mathbf{e}_0 - \mathbf{\Delta}_0(2\mathbf{S}_{1,0}\mathbf{X}_1\mathbf{e}_1).$$

As  $\mathbf{S}_{1,0} = \mathbf{0}$  we get  $\mathbf{C}_{0,0}\mathbf{e}_0 = y_{r0} - 2\mathbf{C}_{1,0}\mathbf{e}_1$ . Substituting this in equation 15, we get

$$\mathbf{y}_r - \mathbf{1}y_{r0} = 2(\mathbf{C}_1 - \mathbf{\Delta}\mathbf{C}_{1,0})\mathbf{e}_1 - 2\mathbf{\Delta}\mathbf{S}_1\mathbf{X}_1\mathbf{e}_1$$

where  $\mathbf{1}$  is a column vector of 1s. Define the quantities

$$\begin{aligned} \mathbf{C}_r &= 2(\mathbf{C}_1 - \mathbf{\Delta}\mathbf{C}_{1,0}), & \mathbf{S}_r &= \mathbf{S}_c = 2\mathbf{S}_1, \\ \mathbf{C}_c &= 2\mathbf{C}_1, & \mathbf{a} &= \mathbf{y}_r - \mathbf{1}y_{r0}, & \mathbf{b} &= \mathbf{y}_c. \end{aligned}$$

$$\text{Further, write } \mathbf{a} = \begin{bmatrix} \mathbf{a}_{-1} \\ \mathbf{0} \\ \mathbf{a}_1 \end{bmatrix}, \mathbf{b} = \begin{bmatrix} \mathbf{b}_{-1} \\ \mathbf{b}_0 \\ -\mathbf{b}_1 \end{bmatrix} \text{ and}$$

$$\mathbf{\Delta} = \begin{bmatrix} \mathbf{\Delta}_{-1} & \mathbf{0} & \mathbf{0} \\ \mathbf{0} & \mathbf{\Delta}_0 & \mathbf{0} \\ \mathbf{0} & \mathbf{0} & \mathbf{\Delta}_1 \end{bmatrix}. \text{ We then obtain the reduced set of equations:}$$

$$\mathbf{a}_{-1} = \mathbf{C}_{r,-1}\mathbf{e}_1 - \mathbf{\Delta}_{-1}\mathbf{S}_{r,-1}\mathbf{X}_1\mathbf{e}_1 \quad (16)$$

$$\mathbf{a}_1 = \mathbf{C}_{r,1}\mathbf{e}_1 - \mathbf{\Delta}_1\mathbf{S}_{r,1}\mathbf{X}_1\mathbf{e}_1 \quad (17)$$

$$\mathbf{b}_{-1} = \mathbf{S}_{c,-1}\mathbf{o}_1 + \mathbf{\Delta}_{-1}\mathbf{C}_{c,-1}\mathbf{X}_1\mathbf{o}_1 \quad (18)$$

$$-\mathbf{b}_1 = \mathbf{S}_{c,1}\mathbf{o}_1 + \mathbf{\Delta}_1\mathbf{C}_{c,1}\mathbf{X}_1\mathbf{o}_1 \quad (19)$$

where  $\mathbf{C}_{r,-1} = \mathbf{C}_{r,1}$ ,  $\mathbf{S}_{r,-1} = -\mathbf{S}_{r,1}$ ,  $\mathbf{C}_{c,-1} = \mathbf{C}_{c,1}$  and  $\mathbf{S}_{c,-1} = -\mathbf{S}_{c,1}$ . Ergo,

$$\mathbf{a}_1 - \mathbf{a}_{-1} = -(\mathbf{\Delta}_1 + \mathbf{\Delta}_{-1})\mathbf{S}_{r,1}\mathbf{X}_1\mathbf{e}_1$$

$$\mathbf{b}_1 - \mathbf{b}_{-1} = -(\mathbf{\Delta}_1 + \mathbf{\Delta}_{-1})\mathbf{C}_{c,1}\mathbf{X}_1\mathbf{o}_1.$$

$$\text{Let } \mathbf{\Sigma} = -(\mathbf{\Delta}_1 + \mathbf{\Delta}_{-1})$$

$$\implies \mathbf{S}_{r,1}\mathbf{X}_1\mathbf{e}_1 = \mathbf{\Sigma}^{-1}(\mathbf{a}_1 - \mathbf{a}_{-1}) \quad (20)$$

$$\mathbf{C}_{c,1}\mathbf{X}_1\mathbf{o}_1 = \mathbf{\Sigma}^{-1}(\mathbf{b}_1 - \mathbf{b}_{-1}). \quad (21)$$

It can be verified that the assumption (c) in the theorem is equivalent to presuming that  $\mathbf{\Delta}_{-1,k} \neq -\mathbf{\Delta}_{1,k}$  for any diagonal component  $k$  and thus  $\mathbf{\Sigma}$  is invertible. Since  $\mathbf{\Sigma}$  is diagonal we have

$$\begin{aligned} \mathbf{S}_{r,1}\mathbf{X}_1\mathbf{e}_1 &= \text{diag}(\mathbf{a}_1 - \mathbf{a}_{-1})\text{diag}(\mathbf{b}_1 - \mathbf{b}_{-1})^{-1}\mathbf{\Sigma}^{-1}(\mathbf{b}_1 - \mathbf{b}_{-1}) \\ &= \text{diag}(\mathbf{a}_1 - \mathbf{a}_{-1})\text{diag}(\mathbf{b}_1 - \mathbf{b}_{-1})^{-1}\mathbf{C}_{c,1}\mathbf{X}_1\mathbf{o}_1 \\ &= \mathbf{Z}\mathbf{C}_{c,1}\mathbf{X}_1\mathbf{o}_1 \end{aligned} \quad (22)$$

where  $\mathbf{Z} = \text{diag}(\mathbf{a}_1 - \mathbf{a}_{-1})\text{diag}(\mathbf{b}_1 - \mathbf{b}_{-1})^{-1}$ . As both  $\mathbf{Z}$  and  $\mathbf{\Delta}_{-1}$  are diagonal matrices, they commute and we get

$$\mathbf{\Delta}_{-1}\mathbf{S}_{r,1}\mathbf{X}_1\mathbf{e}_1 = \mathbf{Z}\mathbf{\Delta}_{-1}\mathbf{C}_{c,1}\mathbf{X}_1\mathbf{o}_1 = \mathbf{Z}[\mathbf{b}_{-1} + \mathbf{S}_{c,1}\mathbf{o}_1]$$

where the last equality follows from equation 18 and the relation  $\mathbf{S}_{c,-1} = -\mathbf{S}_{c,1}$ . Substituting in equation 16 gives us:

$$\mathbf{a}_{-1} = \mathbf{C}_{r,1}\mathbf{e}_1 + \mathbf{Z}\mathbf{b}_{-1} + \mathbf{Z}\mathbf{S}_{c,1}\mathbf{o}_1 \quad (23)$$

$$\implies \mathbf{a}_{-1} - \mathbf{Z}\mathbf{b}_{-1} = \mathbf{C}_{r,1}\mathbf{e}_1 + \mathbf{Z}\mathbf{S}_{c,1}\mathbf{o}_1. \quad (24)$$

Consider equations 22 and 23. These can be written in matrix form as:

$$\begin{bmatrix} \mathbf{a}_{-1} - \mathbf{Z}\mathbf{b}_{-1} \\ \mathbf{0} \end{bmatrix} = \begin{bmatrix} \mathbf{C}_{r,1} & \mathbf{Z}\mathbf{S}_{c,1} \\ \mathbf{S}_{r,1}\mathbf{X}_1 & -\mathbf{Z}\mathbf{C}_{c,1}\mathbf{X}_1 \end{bmatrix} \begin{bmatrix} \mathbf{e}_1 \\ \mathbf{o}_1 \end{bmatrix}. \quad (25)$$

This is of the form  $\mathbf{g} = \mathbf{H}\mathbf{w}$ , with

$$\mathbf{g} \triangleq \begin{bmatrix} \mathbf{a}_{-1} - \mathbf{Z}\mathbf{b}_{-1} \\ \mathbf{0} \end{bmatrix}, \mathbf{H} \triangleq \begin{bmatrix} \mathbf{C}_{r,1} & \mathbf{Z}\mathbf{S}_{c,1} \\ \mathbf{S}_{r,1}\mathbf{X}_1 & -\mathbf{Z}\mathbf{C}_{c,1}\mathbf{X}_1 \end{bmatrix}, \mathbf{w} \triangleq \begin{bmatrix} \mathbf{e}_1 \\ \mathbf{o}_1 \end{bmatrix}.$$

Using this linear system of equations, we can recover  $\mathbf{w}$ . With  $M = N$ , this is a simple case of inverting the  $\mathbf{H}$  matrix. For  $M < N$ , we can invoke results from compressed sensing literature. If  $\mathbf{x}$  is  $s$ -sparse, the vector  $\mathbf{w}$  can easily be shown to be  $2s$ -sparse.

Since  $\mathbf{w} = \begin{bmatrix} \mathbf{e}_1 \\ \mathbf{o}_1 \end{bmatrix}$ , recovering  $\mathbf{w}$  immediately gives us the signal  $\mathbf{x}$ . If  $M = N$ , the applicability of the previous results hinges on the invertibility of  $\mathbf{H}$ . We can show that  $\mathbf{e}_1$  and  $\mathbf{o}_1$  are indeed necessarily recoverable from this linear system.

Consider the second set of equations in equation 25. i.e.  $\mathbf{S}_{r,1}\mathbf{X}_1\mathbf{e}_1 = \mathbf{Z}\mathbf{C}_{c,1}\mathbf{X}_1\mathbf{o}_1$ , which implies that

$$\mathbf{e}_1 = \mathbf{X}_1^{-1}\mathbf{S}_{r,1}^{-1}\mathbf{Z}\mathbf{C}_{c,1}\mathbf{X}_1\mathbf{o}_1. \quad (26)$$

All the matrices involved here are composed of elementary entries and are invertible because of the properties of the Fourier matrix. Substituting this value of  $\mathbf{e}_1$  in the first set of equations in 25, we get

$$\mathbf{a}_{-1} - \mathbf{Z}\mathbf{b}_{-1} = [\mathbf{C}_{r,1}\mathbf{X}_1^{-1}\mathbf{S}_{r,1}^{-1}\mathbf{Z}\mathbf{C}_{c,1}\mathbf{X}_1 + \mathbf{Z}\mathbf{S}_{c,1}]\mathbf{o}_1 \quad (27)$$

$$\implies \mathbf{S}_{c,1}^{-1}\mathbf{Z}^{-1}(\mathbf{a}_{-1} - \mathbf{Z}\mathbf{b}_{-1}) = (\mathbf{E} + \mathbf{I})\mathbf{o}_1, \quad (28)$$

where

$$\mathbf{E} = \mathbf{S}_{c,1}^{-1} \mathbf{Z}^{-1} \mathbf{C}_{r,1} \mathbf{X}_1^{-1} \mathbf{S}_{r,1}^{-1} \mathbf{Z} \mathbf{C}_{c,1} \mathbf{X}_1.$$

Let  $\mathbf{A} = \mathbf{I}$ ,  $\mathbf{U} = \mathbf{S}_{c,1}^{-1} \mathbf{Z}^{-1}$ ,  $\mathbf{C} = \mathbf{C}_{r,1} \mathbf{X}_1^{-1} \mathbf{S}_{r,1}^{-1}$ ,  $\mathbf{V} = \mathbf{Z} \mathbf{C}_{c,1} \mathbf{X}_1$ .

Then  $\mathbf{E} + \mathbf{I} = \mathbf{A} + \mathbf{UCV}$ . The measurement  $\mathbf{Z}$  is independent of both  $\mathbf{A}$  and  $\mathbf{C}$ . For the matrix  $\mathbf{E} + \mathbf{I}$  to not be invertible, we would need to select a precise  $\mathbf{Z}$ , so as to get an eigenvalue of  $-1$  for  $\mathbf{E}$ . Given that the perturbations are picked uniformly at random, the matrix is invertible with probability 1.

This shows that using the approximation as described, the signal  $\mathbf{x}$  is recoverable uniquely when  $M = N$ . While we haven't shown a bound in a compressed sensing framework, where  $M < N$ , we have empirically observed that recovery is excellent in this scenario as well. Empirically, we observe good recovery with this formulation, even with row-sampled Fourier matrix ( $M \leq N$ ). The variation of the error is presented for a 20-sparse signal of length 100 in figure 9. The reported error is with respect to measurements taken in a Taylor approximation forward model, where the Lagrange remainder is assumed to be zero, and do not reflect the recovery error introduced by the Taylor approximation.

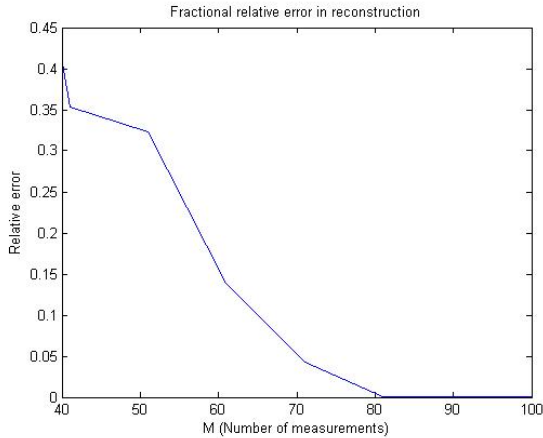


Figure 9. Relative recovery error using linearized model formulation

### C. Bound on Recovery in Expectation

We now show a bound on recovery accuracy using a simplified form of the proposed algorithm in the expected case. The bound invokes results and proof methodology from [9]. Assuming the frequency perturbations are i.i.d., picked from  $\text{Unif}[-r, +r]$ , consider the expected measurement from the system  $\mathbf{F}_t \mathbf{x} + \epsilon$ . That is,

$$\tilde{\mathbf{y}} = \mathbb{E}_\Delta[\mathbf{y}] + \epsilon = \mathbb{E}_\Delta[\mathbf{F}_t \mathbf{x}] + \epsilon.$$

Since each perturbation  $\Delta_k$  is assumed to be independent, we can calculate the value of  $\mathbb{E}_{\Delta_k}[(\mathbf{F}_t \mathbf{x})_k]$ .

$$\begin{aligned} \mathbb{E}_{\Delta_k}[(\mathbf{F}_t \mathbf{x})_k] &= \mathbb{E}_{\Delta_k} \left[ \frac{1}{\sqrt{M}} \sum_j \exp\left(\frac{-2\pi i j (u_k + \Delta_k)}{N}\right) \mathbf{x}_j \right] \\ &= \mathbb{E}_{\Delta_k} \left[ \frac{1}{\sqrt{M}} \sum_j \exp\left(\frac{-2\pi i j u_k}{N}\right) \mathbf{x}_j \exp\left(\frac{-2\pi i j \Delta_k}{N}\right) \right] \\ &= \left[ \frac{1}{\sqrt{M}} \sum_j \exp\left(\frac{-2\pi i j u_k}{N}\right) \mathbf{x}_j \frac{\sin \frac{2\pi j r}{N}}{\frac{2\pi j r}{N}} \right]. \end{aligned}$$

The last equality follows the steps from Section V-A. Defining  $\mathbf{G}$  to be a diagonal matrix such that

$$\mathbf{G}_{jj} = \frac{\sin \frac{2\pi j r}{N}}{\frac{2\pi j r}{N}}, \text{ we can see that}$$

$$\mathbb{E}_\Delta[\mathbf{F}_t \mathbf{x}] = \mathbf{F} \mathbf{G} \mathbf{x}. \quad (29)$$

Using this result, we can concretely state the recovery bound in the following theorem:

*Theorem 3:* Let

$$\tilde{\mathbf{y}} = \mathbf{F} \mathbf{G} \mathbf{x} + \epsilon$$

and  $\mathbf{x}^*$  be the solution to the recovery problem

$$\begin{aligned} \min \quad & \|\mathbf{x}\|_1 \\ \text{s.t.} \quad & \|\tilde{\mathbf{y}} - \mathbf{F} \mathbf{x}\| \leq \epsilon' \end{aligned}$$

where  $\mathbf{F}$  is the Fourier matrix at unperturbed frequencies. Under mild conditions of  $\mathbf{F}$  and  $\mathbf{x}$  as assumed in Theorem 2 of [9], there exists a suitable value of  $\epsilon'$  and constants  $C_0, C_1$ , for which the recovery error is bounded as:

$$\|\mathbf{x}^* - \mathbf{x}\|_2 \leq \frac{C_0}{\sqrt{s}} \|\mathbf{x} - \mathbf{x}_{(s)}\|_2 + C_1 \epsilon'$$

where  $\mathbf{x}_{(s)}$  is the best  $s$ -term approximation of  $\mathbf{x}$  containing the largest  $s$  coefficients of  $\mathbf{x}$  with the rest set to zero.

We now prove this result drawing upon a proof from Theorem 2 of [9], to which our formulation is analogous. To see the analogy more clearly, we define the following quantities:

$$\begin{aligned} \mathbf{E} &:= \mathbf{F}(\mathbf{G} - \mathbf{I}) \quad \text{and} \\ \epsilon_F &:= \|\mathbf{G} - \mathbf{I}\|_2, \end{aligned}$$

$\|\mathbf{F}\|_2$  equals the largest singular value of a matrix  $\mathbf{F}$ . Let  $\|\mathbf{F}\|_2^{(s)}$  denotes the largest singular value taken over all  $s$ -column submatrices of  $\mathbf{F}$ . We have

$$\frac{\|\mathbf{E}\|_2}{\|\mathbf{F}\|_2} \leq \frac{\|\mathbf{F}\|_2 \|\mathbf{G} - \mathbf{I}\|_2}{\|\mathbf{F}\|_2} = \|\mathbf{G} - \mathbf{I}\|_2 = \epsilon_F. \quad (30)$$

Further, since  $\mathbf{G}$  and  $\mathbf{I}$  are both diagonal matrices, multiplication by  $(\mathbf{G} - \mathbf{I})$  conserves the sparsity of any signal  $s$ -sparse signal  $\mathbf{x}_s$ . Therefore,  $\|\mathbf{E}\|_2^{(s)} \leq \|\mathbf{F}\|_2^{(s)} \|\mathbf{G} - \mathbf{I}\|_2$  and hence  $\frac{\|\mathbf{E}\|_2^{(s)}}{\|\mathbf{F}\|_2^{(s)}} \leq \epsilon_F$ . From here we can follow exactly along the

proof lines of Theorem 2 in [9], and arrive at a value of  $\epsilon'$  (see Eqn. 14 of [9]) satisfying  $\|\tilde{\mathbf{y}} - \mathbf{F}\mathbf{x}\| \leq \epsilon'$  given that  $\|\tilde{\mathbf{y}} - \mathbf{F}\mathbf{G}\mathbf{x}\| = \|\epsilon\| \leq \epsilon$  and the constants  $C_0$  and  $C_1$  to derive the bound stated in our Theorem 3.

Note that this minimization problem does not account for the actual matrix  $\mathbf{F}_t$  being known or even estimated during the recovery process. In practice, using the algorithm we have proposed in section III, the matrix  $\mathbf{\Delta}$  (and hence  $\mathbf{F}_t$ ) is estimated at each step, and the recovery is realistically, much better than the bound arrived at using the approach above. In future work, we hope to be able to also provide a bound for this scenario where  $\mathbf{F}_t$  is estimated.

## VI. CONCLUSIONS AND DISCUSSION

We have presented a method to correct for perturbations in a Fourier matrix *in situ* during signal reconstruction. Our method is simple to implement, robust to noise and well grounded in theory. We have shown a theoretical analysis of approximations to the basic problem as well. We have consciously avoided using a Taylor approximation for the algorithm presented unlike [10], [11], even though it simplifies the problem considerably. This is to avoid introduction of modeling error due to the Lagrange remainder term which can be quite significant except at small values of  $r$ . At low levels of perturbation (small  $r$ ), the Taylor error can be ignored. However, if the perturbation is small, we have observed that comparable results can be obtained by simply ignoring the perturbation in the measurement matrix (i.e. setting  $\delta = 0$ ), for the specific computational problem that this paper deals with. In fact, it was verified using simulated data that for  $r < 1$ , Taylor approximation methods barely outperformed simple basis pursuit (which considers the model  $\mathbf{y} = \mathbf{F}\mathbf{x} + \boldsymbol{\eta}$ , and recovers only  $\mathbf{x}$ ), if at all. For larger perturbations, the Taylor noise is too overwhelming to be ignored and the recovery error in tests conducted using such a framework was found to be unacceptably high. The method proposed here comfortably outperforms even an oracular solution to the system obtained by Taylor approximation.

Future work will involve exploration of applications in MRI and DOA estimation. There also exist two compelling theoretical issues that are still open - (1) formally establishing the uniqueness of the joint solution of  $(\mathbf{x}, \boldsymbol{\delta})$  from perturbed measurements for  $M \leq N$ , and (2) derivation of error bounds on the estimates of  $(\mathbf{x}, \boldsymbol{\delta})$  for the case of compressed sensing with perturbed Fourier matrices.

## REFERENCES

- [1] E. Candès and M. Wakin, "An introduction to compressive sampling," *IEEE signal processing magazine*, vol. 25, no. 2, pp. 21–30, 2008.
- [2] O. Katz, J. M. Levitt, and Y. Silberberg, "Compressive fourier transform spectroscopy." Optical Society of America, 2010.
- [3] P. Schniter and S. Rangan, "Compressive phase retrieval via generalized approximate message passing," *IEEE Trans. Signal Processing*, vol. 63, no. 4, pp. 1043–1055, 2015. [Online]. Available: <https://doi.org/10.1109/TSP.2014.2386294>
- [4] M. Lustig, "Compressed sensing MRI," *IEEE Signal Processing Magazine*, 2008.
- [5] L. C. Potter, E. Ertin, J. T. Parker, and M. Çetin, "Sparsity and compressed sensing in radar imaging," *Proceedings of the IEEE*, vol. 98, no. 6, pp. 1006–1020, 2010.

- [6] H. Jang and A. B. McMillan, "A rapid and robust gradient measurement technique using dynamic single-point imaging," *Magnetic Resonance in Medicine*, 2016.
- [7] R. K. Robison, A. Devaraj, and J. G. Pipe, "Fast, simple gradient delay estimation for spiral MRI," *Magnetic resonance in medicine*, vol. 63, no. 6, pp. 1683–1690, 2010.
- [8] E. Brodsky, A. Samsonov, and W. Block, "Characterizing and correcting gradient errors in non-cartesian imaging: Are gradient errors linear-time-invariant?" *Magnetic Resonance Imaging*, vol. 62, pp. 1466–1476, 2009.
- [9] M. A. Herman and T. Strohmer, "General deviants: An analysis of perturbations in compressed sensing," *J. Sel. Topics Signal Processing*, vol. 4, no. 2, pp. 342–349, 2010.
- [10] Z. Yang, C. Zhang, and L. Xie, "Robustly stable signal recovery in compressed sensing with structured matrix perturbation," *IEEE Transactions on Signal Processing*, vol. 60, no. 9, pp. 4658–4671, 2012.
- [11] T. Zhao, Y. Peng, and A. Nehorai, "Joint sparse recovery method for compressed sensing with structured dictionary mismatches," *IEEE Transactions on Signal Processing*, vol. 62, no. 19, pp. 4997–5008, 2014.
- [12] H. Zhu, G. Leus, and G. Giannakis, "Sparsity-cognizant total least-squares for perturbed compressive sampling," *IEEE Transactions on Signal Processing*, vol. 59, 2011.
- [13] S. Ling and T. Strohmer, "Self-calibration via linear least squares," *CoRR*, vol. abs/1611.04196, 2016. [Online]. Available: <http://arxiv.org/abs/1611.04196>
- [14] —, "Self-calibration and biconvex compressive sensing," *Inverse Problems*, vol. 31, 2015.
- [15] C. Bilen, G. Puy, R. Gribonval, and L. Daudet, "Convex optimization approaches for blind sensor calibration using sparsity," *IEEE Transactions on Signal Processing*, vol. 62, no. 8, pp. 4847–4856, 2014.
- [16] V. Cambareri and L. Jacques, "A non-convex blind calibration method for randomised sensing strategies," in *4th International Workshop on Compressed Sensing Theory and its Applications to Radar, Sonar and Remote Sensing (CoSeRa)*, 2016, p. 1620.
- [17] Y. Chi, L. L. Scharf, A. Pezeshki, and A. R. Calderbank, "Sensitivity to basis mismatch in compressed sensing," *IEEE Trans. Signal Processing*, vol. 59, no. 5, pp. 2182–2195, 2011.
- [18] J. M. Nichols, A. K. Oh, and R. M. Willett, "Reducing basis mismatch in harmonic signal recovery via alternating convex search," *IEEE Signal Process. Lett.*, vol. 21, no. 8, pp. 1007–1011, 2014.
- [19] G. Tang, B. N. Bhaskar, P. Shah, and B. Recht, "Compressed sensing off the grid," *IEEE Trans. Information Theory*, vol. 59, no. 11, pp. 7465–7490, 2013.
- [20] A. Aldroubi, X. Chen, and A. M. Powell, "Perturbations of measurement matrices and dictionaries in compressed sensing," *Applied and Computational Harmonic Analysis*, vol. 33, no. 2, pp. 282–291, 2012.
- [21] J. D. Ianni and W. A. Grissom, "Trajectory auto-corrected image reconstruction," *Magnetic resonance in medicine*, vol. 76, no. 3, pp. 757–768, 2016.
- [22] M. Ferrucci, R. Leach, C. Giusca, S. Carmignato, and W. Dewulf, "Towards geometrical calibration of X-ray computed tomography systems: a review," *Measurement Science and Technology*, vol. 26, no. 9, p. 092003, 2015.
- [23] S. Basu and Y. Bresler, "Uniqueness of tomography with unknown view angles," *IEEE Transactions on Image Processing*, vol. 9, no. 6, pp. 1094–1106, 2000.
- [24] Y. Fang, M. Sun, S. Vishwanathan, and K. Ramani, "sLLE: Spherical locally linear embedding with applications to tomography," in *Computer Vision and Pattern Recognition (CVPR), 2011 IEEE Conference on*. IEEE, 2011, pp. 1129–1136.
- [25] E. Malhotra and A. Rajwade, "Tomographic reconstruction from projections with unknown view angles exploiting moment-based relationships," in *ICIP*, 2016, pp. 1759–1763.
- [26] A. Belloni, V. Chernozhukov, and L. Wang, "Square-root LASSO: pivotal recovery of sparse signals via conic programming," *Biometrika*, vol. 98, no. 4, p. 791, 2011.
- [27] D. L. Donoho and M. Elad, "Optimally sparse representation in general (nonorthogonal) dictionaries via  $\ell_1$  minimization," *Proceedings of the National Academy of Sciences*, vol. 100, no. 5, pp. 2197–2202, 2003.
- [28] C. Studer and R. Baraniuk, "Stable restoration and separation of approximately sparse signals," *Applied and Computational Harmonic Analysis*, vol. 37, no. 1, pp. 12–35, 2014.